(Zabicky, J., Ed.) p 754, Wiley, New York.
Changeux, J.-P., Devillier-Thiéry, A., & Chemouilli, P. (1983) *Science (Washington, D.C.) 225*, 1335–1345.
Delcour, A. H., & Hess, G. P. (1986) *Biochemistry* (preceding paper in this issue).
Delcour, A., Cash, D. J., Erlanger, B., & Hess, G. P. (1982) *J. Chromatogr. 248*, 461–468.
Doulakas, J. (1975) *Pharm. Acta Helv. 50*, 447–450.
Engels, J., & Schlaeger, E. J. (1977) *J. Med. Chem. 20*, 907–911.
Goldman, Y. E., Hibberd, M. G., McCray, J. A., & Trentham, D. R. (1982) *Nature (London) 300*, 701–705.
Goldman, Y. E., Hibberd, M. G., & Trentham, D. R. (1984) *J. Physol. (London) 354*, 577–604.
Hess, G. P., Cash, D. J., & Aoishima, H. (1979) *Nature (London) 282*, 329–331.
Hess, G. P., Cash, D. J. & Aoshima, H. (1983) *Annu. Rev. Biophys. Bioeng. 12*, 443–473.
Kaplan, J. N., Forbush, B., & Hoffman, J. F. (1978) *Biochemistry 17*, 1929–1935.
Lester, H. A., & Nerbonne, J. M. (1982) *Annu. Rev. Biophys. Bioeng. 11*, 151–175.
McCray, J. A., Herbette, L., Kihara, T., & Trentham, D. R. (1980) *Proc. Natl. Acad. Sci. U.S.A. 77*, 7237–7241.
Morrison, H. A. (1969) in *The Chemistry of the Nitro and Nitroso Groups* (Feuer, H., Ed.) Part 1, pp 165–213, Wiley, New York.
Nerbonne, J. M., Richard, S., Margeot, J., & Lester, H. A. (1984) *Nature (London) 310*, 74–76.
Neubig, R. R., & Cohen, J. B. (1980) *Biochemistry 19*, 2770–2779.
Patchornik, A., Amit, B., & Woodward, R. B. (1970) *J. Am. Chem. Soc. 92*, 6333–6335.
Pillai, V. N. R. (1980) *Synthesis 1*, 1–26.
Rich, D. H., & Gurwara, S. K. (1975) *J. Am. Chem. Soc. 97*, 1575–1578.
Schiffman, G., Kabat, E. A., & Thompson, W. (1964) *Biochemistry 3*, 113–120.
Sprinson, D. B. (1941) *J. Am. Chem. Soc. 63*, 2249.
Tapuhi, Y., & Grushka, E. (1982) in *Chemistry of Amino, Nitroso and Nitro Compounds and Their Derivatives* (Patai, S., Ed.) p 915, Wiley, New York.
Walker, J. W., Lucas, R. J., & McNamee, M. G. (1981a) *Biochemistry 20*, 2191–2199.
Walker, J. W., McNamee, M. G., Pasquale, E., Cash, D. J., & Hess, G. P. (1981b) *Biochem. Biophys. Res. Commun. 100*, 86–90.
Walker, J. W., Takeyasu, K., & McNamee, M. G. (1982) *Biochemistry 21*, 5384–5389.
Wettermark, G. (1962) *J. Phys. Chem. 66*, 2560–2562.

Anisotropy Decay Associated Fluorescence Spectra and Analysis of Rotational Heterogeneity. 1. Theory and Applications†

Jay R. Knutson,‡ Lesley Davenport,§ and Ludwig Brand*
Biology Department and McCollum-Pratt Institute, The Johns Hopkins University, Baltimore, Maryland 21218
Received August 22, 1985

ABSTRACT: Individual fluorescence spectra for species in a heterogeneous system can be determined by using differences between the rotational correlation times of those components. Each spectrum derived is associated with a particular fluorescence anisotropy decay function; hence, they are anisotropy decay associated spectra (ADAS). We have previously shown [Knutson, J. R., Walbridge, D. G., & Brand, L. (1982) *Biochemistry 21*, 4671–4679] that a system containing different decay functions for total intensity can be resolved into constituent decay-associated spectra. ADAS extends the technique into the realm of fluorescence polarization, making use of the often disparate Brownian rotations found in heterogeneous biochemical systems. In this paper, we present the basic theory for ADAS in various heterogeneous systems and then present an example of ADAS resolving a binary mixture of macromolecules into "fast-rotor" (smaller or more mobile) and "slow-rotor" (larger or less mobile) components. They correctly superimpose spectra taken for the unmixed components. In the companion paper [Davenport, L., Knutson, J. R., & Brand, L. (1986) *Biochemistry* (following paper in this issue)], a specific application to a problem of importance of lipid biochemistry—e.g., the origin of the membrane probe order parameter in lipid bilayers—is presented, demonstrating the role rotational heterogeneity may play in biochemical fluorescence.

The Brownian rotations of both small molecules and macromolecules are of key importance in biochemistry. A number of biophysical techniques have been used to provide data about these motions; each, in turn, helps characterize either the size and shape of rotors or the local angular constraints of the molecular environment.

Among the biophysical techniques used to study macromolecules, fluorescence polarization has been especially useful. The historic work of Perrin (1934, 1936) framed a relationship between the lifetime-averaged depolarization process and hydrodynamic (Stokes–Einstein) parameters. These relationships between size, shape, viscosity, temperature, and lifetime have been widely used in biochemistry. The use of extrinsic labels to characterize proteins was spearheaded by Weber and co-workers (Weber, 1952, 1953a,b, 1973). In order

† This work was supported by National Institutes of Health Grant GM 11632. Contribution No. 1305 from the McCollum-Pratt Institute.
‡ Present address: Laboratory of Technical Development, NHLBI, National Institutes of Health, Bethesda, MD 20205.
§ Present address: Chemistry Department, The City University of New York, Brooklyn College, Brooklyn, NY 11210.

0006-2960/86/0425-1805$01.50/0

to simplify polarization, Jablonski (1960) suggested the adoption of a *linear* parameter, r, the fluorescence anisotropy. The linearity of r makes heterogeneity easier to analyze. Most models for complex anisotropy have involved *homogeneous* concepts of segmental, asymmetric, or hindered rotation (Munro et al., 1979; Zannoni, 1981; Lipari & Szabo, 1980; Chuang & Eisenthal, 1972; Kinosita, 1977). These models have done a great deal to extend the theory of polarized fluorescence, yet they do not exploit the powerful *multidimensional* nature of fluorescence. This multidimensional approach was used in early studies by Weber (1961) and Ainsworth (1961), who arranged matrix rank analyses for total intensity on excitation/emission wavelength axes. These methods can identify both the number of species and the spectra (under favorable circumstances) in a mixture. More recently, Halvorson (1981) extended the method via significant factor analysis. In absorption and luminescence problems, the related singular value decomposition (SVD)[1] method is becoming popular (Schrager & Hendler, 1982).

In time-resolved spectroscopy, Donzel et al. (1974) pioneered the extraction of what are now called decay-associated spectra, using the fractional intensities of decay curves at multiple, discrete wavelengths. The explicit separability of the wavelength and time variables for each species was used by Knutson et al. (1982a) to develop alternative schemes for DAS, using rapid collections and matrix inversion for analysis. Recently, "global analysis" (Knutson et al., 1983; Beechem et al., 1983a,b, 1984a, 1985a) has been used to derive DAS from complete analysis of emission data surfaces.

In phase fluorometry, Lakowicz and Cherek (1981) developed a rapid method to separate binary systems (when one phase angle can be found). More recent advances in phase instrumentation (Gratton et al., 1984a) have made multipoint time-resolved spectra available (Gratton et al., 1984b; Lakowicz et al., 1984). A method to extract *multiple* smooth DAS from phase-resolved data has been outlined (Knutson et al., 1982a). It can also be used in cases where global analysis provides more than two characteristic phases (Beechem et al., 1983b). The time and frequency domain methods mentioned so far have all dealt with the decay of *total* intensity (e.g., mixtures of fluorophores with differing lifetimes). In this paper, a procedure is described to resolve spectra in a mixture of differently *rotating* species, without regard to whether the lifetimes differ or not. The procedure associates unique spectra with the anisotropy decay function of each species. Preliminary accounts of this work have been presented elsewhere (Knutson et al., 1982b; Davenport et al., 1982; Brand et al., 1985).

Theory

The theory of ADAS is qualitatively similar to that described in Knutson et al. (1982a), except for the substitution of polarized difference decay functions in place of total decay functions. The substitution follows rearrangement of the anisotropy function for a homogeneous population:

$$r_i(t) = \left[\frac{I_V(t) - I_H(t)}{I_V(t) + 2I_H(t)}\right]_i = \frac{y_i(t)}{d_i(t)} \tag{1}$$

where $I_{parallel} = I_V$ and $I_{perpendicular} = I_H$. This implies that

$$y_i(t) = d_i(t)r_i(t)$$

where $y_i(t)$ is the difference decay function, $d_i(t)$ is the total decay function, and $r_i(t)$ is anisotropy, all for the ith homogeneous component. The nomenclature used is consistent with theory presented elsewhere (Knutson et al., 1982).

For a heterogeneous system, the linearity property of r yields

$$\bar{r}(\lambda,t) = \frac{\sum_{i=1}^{n}\alpha_i(\lambda)d_i(t)r_i(t)}{\sum_{i=1}^{n}\alpha_i(\lambda)d_i(t)} = \frac{\bar{y}(\lambda,t)}{\bar{d}(\lambda,t)} \tag{2}$$

where a bar indicates a heterogeneous sum and where index i enumerates the n species present. In accordance with the theory presented by Knutson et al. (1982), $\alpha_i(\lambda)$ represent the spectra of each component and is *associated* with the proper total intensity and/or anisotropy decay functions through the index i. The numerator of eq 2 provides the mixing information we need to obtain ADAS, $\alpha_i(\lambda)$:

$$\bar{y}(\lambda,t) = \sum_{i=1}^{n}\alpha_i(\lambda)y_i(t) \tag{3}$$

If we measure these difference TRES $\bar{y}(\lambda,t)$ at n or more different times (t_j), we obtain the matrix equation

$$\bar{y} = \mathbf{M}\alpha \tag{4}$$

or

$$\bar{y}(\lambda,t) = \sum_{i=1}^{n}y_i(t_j)\alpha_i(\lambda) \tag{5}$$

where

$$\mathbf{M}_{ij} = y_i(t_j)$$

Since we know the y_i ($=d_ir_i$) functions for all t_j, we know $\mathbf{M}$ and can invert that matrix. To obtain the unknown ADAS $\alpha_i(\lambda)$, we simply multiply $\mathbf{G}$ (the inverse of $\mathbf{M}$) by the measured difference TRES $\bar{y}$:

$$\mathbf{G}\bar{y} = \mathbf{GM}\alpha = \alpha \tag{6}$$

or

$$\alpha_1(\lambda) = \sum_k \mathbf{G}_{k1}\bar{y}(\lambda,t_k) \tag{7}$$

The right-hand side is a remixing process; i.e., the correct linear combinations of the measured difference TRES $\bar{y}$ will yield the ADAS of each species, $\alpha_i(\lambda)$.

Since most practical instruments have a finite response characteristic (and TRES are totaled in a span of instrument channels), we must modify eq 7 somewhat:

$$\bar{Y}(\lambda,j) = \sum_{i=1}^{n}\int_{a_j}^{b_j}Y_i(t')dt'\alpha_i(\lambda) \tag{8}$$

where the jth time window extends from a_j to b_j for jth TRES. We have capitalized $\bar{Y}$ and Y_i to indicate that they are difference TRES and decays, respectively, on *instrument* (convolved) time scales:

$$Y_i(t') = \int_0^{t'} y_i(t'-t)L(t)dt \tag{9}$$

where $L(t)$ is the excitation impulse in the system. Notice that convolution of this linear system acts selectively on the time axis. We must simply use convolved (and window summed) mixing coefficients in our mixing matrix:

$$\mathbf{M}_{ij} = \int_{a_j}^{b_j}Y_i(t')dt' \tag{10}$$

[1] Abbreviations: ADAS, anisotropy decay associated spectra; 9-CNA, 9-cyanoanthracene; DAS, decay-associated spectra; EtOH, ethanol; HLADH, horse liver alcohol dehydrogenase (EC 1.1.1.1); TNS, 2-(*p*-toluidino)naphthalene-6-sulfonate; TRES, time-resolved emission spectra; SVD, singular value decomposition.

Then, as before, we can invert **M** to obtain

$$\alpha_l(\lambda) = \sum_k \mathbf{G}_{kl}\bar{Y}(\lambda,k) \tag{11}$$

where α represents the desired ADAS, $\mathbf{G}_{kl}$ is the inverse matrix of **M**, and $\bar{Y}(\lambda,k)$ is the windowed difference TRES, indexed according to window $a_k \rightarrow b_k$ channel intervals. Thus, even in the presence of convolution requirements, one can derive ADAS by properly mixing the measured difference TRES.

Binary Mixture. Suppose a system is comprised of two species having distinct spectra and rotational correlation times. Further suppose the system exhibits binary total emission decay, e.g.

$$\bar{d}(\lambda,t) = [\alpha_1(\lambda)\gamma_{11}e^{-t/\tau_1} + \alpha_1(\lambda)\gamma_{12}e^{-t/\tau_2}] + [\alpha_2(\lambda)\gamma_{21}e^{-t/\tau_1} + \alpha_2(\lambda)\gamma_{22}e^{-t/\tau_2}] = [\alpha_1(\lambda)d_1(t)] + [\alpha_2(\lambda)d_2(t)] \tag{12}$$

where α_i are the characteristic spectra and d_i the characteristic total decays of each (differently rotating) species. Since $y_i = d_i r_i$

$$\bar{y}(\lambda,t) = \alpha_1(\lambda)d_1(t)r_1(t) + \alpha_2(\lambda)d_2(t)r_2(t) \tag{13}$$

where

$$r_i(t) = r_{0_i}e^{-t/\phi_i} \tag{14}$$

is an example for the simplest type of rotational heterogeneity. The form of $d_1(t)$ and $d_2(t)$ determines whether or not the system is *associative*, i.e., whether lifetimes and ϕ values (correlation times) correspond. If so, the system is said to be *associative*:

$$\gamma_{ij} = \delta_{ij} \qquad (1 \text{ for } i = j,\ 0 \text{ otherwise})$$

Nonassociative systems are characterized by lack of τ to ϕ linkage, e.g.

$$\gamma_{ij} = \gamma_j \qquad (\text{independent of } \phi_i,\ \alpha_i)$$

One can classify other forms of the γ_{ij} as "partially" associative. ADAS recovery does not require one form or the other. If the $y_i(t)$ functions in a system can be deduced, ADAS will follow. In our experience, the best method for obtaining the proper y_i is the global analysis methodology developed by Beechem et al. (1984). In many cases, conventional analyses will suffice, but the global programs offer true statistical testing of associative vs. nonassociative models. In many important biological cases, whether or not τ to ϕ associations are present, the differences between d_i may be subtle compared to the dramatic differences found in rotation (and hence y_i). The experimental system to be presented is a typical example of this phenomenon.

An extension of this stark contrast can appear when small molecules either are bound to much larger molecules or are free in solution. In this case, even steady-state methods may be sufficient. To illustrate, consider a simple associative system with monoexponential intensity and anisotropy decays in both free (F) and bound (B) cases:

$$\bar{y}(\lambda,t) = \alpha_B(\lambda)e^{-t/\tau_B}r_{0_B}e^{-t/\phi_B} + \alpha_F(\lambda)e^{-t/\tau_F}r_{0_F}e^{-t/\phi_F} \tag{15}$$

Integrated to form steady-state (ss) differences, this yields

$$\bar{y}(\lambda,\text{ss}) = \int_0^\infty \bar{y}(\lambda,t)\,dt = \frac{\alpha_B(\lambda)r_{0_B}}{1/\tau_B + 1/\phi_B} + \frac{\alpha_F(\lambda)r_{0_F}}{1/\tau_F + 1/\phi_F} \tag{16}$$

Note that

$$\bar{y}(\lambda,\text{ss}) \cong \frac{\alpha_B(\lambda)r_{0_B}}{1/\tau_B + 1/\phi_B} \tag{17}$$

when $\phi_F << (\tau_F \sim \tau_B \sim \phi_B)$. Thus, the steady-state difference spectrum is predominantly the bound spectrum. This is, of course, predicated on a relatively small free rotation time and a yield that does not (anomalously) decrease sharply upon binding. The derived shapes of both free and bound spectra can later be used to determine equilibria. A similar limiting approximation was used by Ermolaev et al. (1982) to extract the small (steady-state) difference spectra contribution of a polarized (short-lived) component from an otherwise depolarized mixture. In their case, $\phi_F \sim \phi_B \sim \tau_B << \tau_F$.

The theory presented so far assumes that r_{0i}, the initial anisotropy of the ith component, is independent of emission wavelength. This is in accord with the Vavilov–Kasha rule (combined with "golden rule" separability) and should hold for most fluorophores. I. Steinberg (personal communication) has pointed out, however, that probes with long natural lifetimes may exhibit state mixing such that r_0 varies with the vibrational band. In addition, excited-state reactions can provide heterogeneous anisotropy spectra (Matayoshi & Kleinfeld, 1979; Knutson & Lakowicz, 1980; Lakowicz, 1984; Cross et al., 1984). In the former case, ADAS would be slightly distorted but would still succeed in resolving any heterogeneity linked to correlation time. If comparisons are made between difference spectra vs. time instead of difference vs. magic angle spectra, no ambiguity is possible. In the second case (excited-state reactions), the variation of $\langle r \rangle$ with λ is exactly the sort of heterogeneity we seek to detect: coexistence of states with different y functions. The functional form of y_i for daughter states includes "history" in the parent state (Knutson & Lakowicz, 1980) and may differ even if ϕ remains the same. This can arise from the trivial effect of delayed emission from the daughter state, or from intramolecular oscillator changes. The use of ADAS in these cases is beyond the scope of this paper; suffice it to say that ADAS methods will correctly detect the presence of heterogeneity, and accompanying DAS will pin down the ground-vs. excited-state heterogeneity. DAS for excited-state reactions (Knutson et al., 1982a; Davenport et al., 1983, 1986; Davenport & Brand, 1985) have been shown to correctly resolve both spectra and the excited-state heritage. Recently, Beechem et al. (1984b, 1985b) have formalized a global approach to directly obtain DAS for the *species* in an excited-state reaction (SAS: species-associated spectra). The latter method has advantages in error propagation and analysis, plus it is more easily generalized to multiple species.

In summary, the theory of ADAS parallels DAS; difference decay functions (y_i) provide the function with which to associate spectra. In the same manner as DAS, identification of these basis functions is facilitated via global analysis, and multiexponential (or nonexponential) functions present no special problem.

The basic principle behind ADAS separations is illustrated schematically in Figure 1. Two different probe populations are excited by a pulse of polarized light; at early times, *both* photoselected ensembles remain partly oriented with the excitation polarization axis z. At later times, both populations are depleted by the same *number*, so total (parallel plus two perpendicular or, equivalently, magic angle) intensity profiles track together. In contrast, one of the populations depolarizes (e.g., via Brownian rotation or transfer) much more rapidly, and the *difference* decays separate.

Experimental Procedures

All spectra and anisotropy decays were collected and analyzed as previously described (Badea & Brand, 1979; Chen et al., 1977). The excitation polarizer was alternated to provide parallel and perpendicular curves, while the emission polarizer

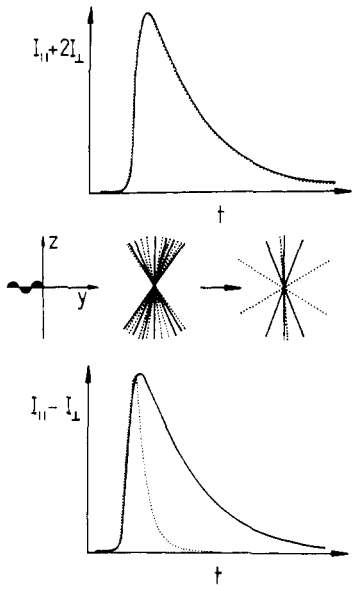

FIGURE 1: Total vs. difference decays of intensity in a rotationally heterogeneous system. Photoselection of probes yields an ordered ensemble of oscillators in the excited (fluorescent) state. The *total* intensity, $I_V + 2I_H$, is independent of orientation and simply reports the loss of excited-state concentration (the same for both populations here) due to decay. Difference decay functions, in contrast, report the simultaneous loss of number *and* polarization. Thus, it drops more rapidly than the total decay for mobile probes (···). Less mobile (slower or more restricted, —) probes have a difference decay more akin to total decay.

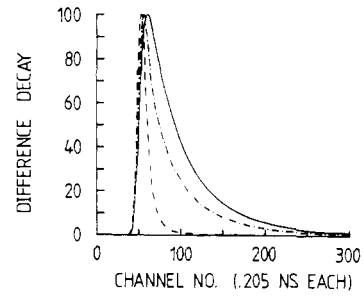

FIGURE 2: Difference decay functions for TNS bound to (– –) β-cyclodextrin (1:1 labeling ratio), (—) HLADH (2:1 probe to protein ratio), and mix (–·–). The polarized difference intensity clearly declines more rapidly for the smaller complex, and the mix curve lies between those of the larger and smaller components. The experimental fluorescence decay curve of the total emission, $d(t)$, for LADH/TNS was best fit to a triple exponential ($f_1 = 0.304$, $\tau_1 = 12.44$ ns, $f_2 = 0.334$, $\tau_2 = 0.97$ ns, $f_3 = 0.362$, $\tau_3 = 5.73$ ns). The χ^2 obtained was 1.78. The parameters obtained for $d(t)$ were used together with the experimental difference curve $Y(t)$ to obtain parameters $r(t)$ in terms of the impulse response model $Y(t) = r(t)d(t)$. $r(t)$ for TNS/LADH was recovered in terms of a single-exponential decay ($\beta = 0.32$, $\phi = 70.71$ ns, $\chi^2 = 1.19$). Similarly, for TNS/cyclodextrin, $f_1 = 0.338$, $\tau_1 = 2.07$ ns, $f_2 = 0.624$, $\tau_2 = 0.58$ ns, $f_3 = 0.038$, and $\tau_3 = 6.71$ ns with $\chi^2 = 2.26$. $r(t)$ was recovered as a single-exponential decay ($\beta = 0.33$, $\phi = 0.36$ ns, and $\chi^2 = 1.26$). Excitation was at 357 nm and emission at 430 nm, with bandwidths of 14 and 16 nm, respectively. The temperature was 10 °C. Values for the steady-state emission anisotropy for TNS/LADH, TNS/cyclodextrin, and TNS/mix were 0.28, 0.095, and 0.193, respectively.

remained vertical. Thus, the polarization impinging on the monochromator/detector train was unchanged, and the G factor (Chen & Bowman, 1965; Badea & Brand, 1979) was invariant with emission wavelength. This was confirmed from a comparison of polarized decays of 9-CNA in EtOH, since this dye's lifetime greatly exceeds its rotation time ($\tau/\phi \gtrsim 100$) and its total anisotropy is well approximated by zero. 9-CNA also served as a lifetime standard for determining the "Q" (or color) shift in detector timing between excitation and emission wavelengths (Badea & Brand, 1979; Wahl, 1969). These values were always small compared to time window intervals (≲200 ps vs. several nanoseconds). Excitation with a nitrogen flashlamp was achieved through a Baird-Atomic interference filter centered on the line at 357 nm, with 14-nm band-pass.

Time-windowed TRES were collected in the same fashion described by Knutson et al. (1982a), with the exception that polarized TRES were collected in alternated scans of identical samples. The parallel TRES was multiplied by the appropriate G factor prior to further processing.

Anisotropy decay functions were analyzed by using the derived G factor and, for comparison, via a program that calculates G from the input value of $\bar{r}$ (steady-state anisotropy). These $\bar{r}$ values were obtained on a Perkin-Elmer MPF 44 (excitation, 357 nm, bandwidth, 14 nm; emission; 430 nm, bandwidth, 7 nm) using Polaroid sheet polarizers.

Horse liver alcohol dehydrogenase (HLADH) was obtained from Boehringer-Mannheim and dialyzed as described by Ross et al. (1980). 2-(*p*-Toluidino)naphthalene-6-sulfonate was obtained from Sigma Chemical Co. HLADH in 0.05 M sodium phosphate buffer at pH 7.4 was added to TNS (which had been evaporated in a round-bottom flask from a 1 mM ethanol solution). A 2:1 ratio of dye to protein was employed. The total enzyme concentration was 5×10^{-6} M. β-Cyclodextrin (Mann Research Laboratories) was recrystallized from ethanol and then labeled with TNS in a similar fashion, except a labeling ratio of 1:1 was used. The unimportance of free TNS fluorescence was verified by examining equivalent TNS/buffer solutions. Since the fluorescence yield for TNS adsorbed to β-cyclodextrin is lower than that adsorbed to protein, labeled samples of HLADH and β-cyclodextrin mixtures were prepared such that the peaks of maximum fluorescence emission for TNS were equivalent when excited at 330 nm. Inner filter effects were avoided by maintaining absorbances <0.10, and total emission decays and spectra used magic-angle configurations to isolate rotational effects [for a review, see Badea & Brand (1979)].

RESULTS

Total fluorescence spectra of TNS/HLADH and TNS/β-cyclodextrin complexes (both separately and mixed) were obtained, along with total (magic-angle) decay functions. Both complexes showed multiexponential decays. The intensity decay constants are given in the legend to Figure 2. Since we were interested in anisotropy rather than lifetime associations, no attempt was made to subdivide the total decay terms and spectral components for these separate complexes. The total intensity decays were similar and sufficiently long-lived to allow adequate time windowing. (The subtle spectral shifts accompanying solvent relaxation of the TNS in each binding site were not at issue here; they are best examined by new global methods.)

Polarized decay curves, $I_V(t)$ and $I_H(t)$, were obtained, and the difference decay curves [$Y = I_V(t) - I_H(t)$] are shown in Figure 2. They are extremely disparate, as one would expect from the comparison of molecular weights (HLADH, $M_r \sim 84\,000$; β-cyclodextrin, $M_r \sim 1135$). The difference decay for the mixture, as predicted, is situtated between these extremes. Thus, this provides a good example of the coexistence of a large rotational rate disparity. The rotational correlation time for the HLADH/TNS complex was 71 ns as compared to 0.4 ns for the cyclodextrin complex. The total intensity decay does not vary strongly between the two complexes. The anisotropy decay functions were obtained from traditional

(nonassociative) analysis at 430 nm. The anisotropy (and hence the difference decay) of β-cyclodextrin complexes is lost rapidly. In this extreme case, a "late" time-windowed polarized difference TRES can be obtained that is virtually devoid of spectral contribution from TNS/cyclodextrin. This feature was used to directly isolate the slow-rotor ADAS seen in Figure 3 (from a *mixture* of TNS/cyclodextrin and TNS/HLADH). As expected, this ADAS superposes the total spectrum of TNS/HLADH taken separately. We note that a window *with* cyclodextrin contributions could have been used, if one had another (e.g., earlier) difference TRES to subtract away. If the difference function areas were not the same in those windows, a simple multiplicative constant would be applied prior to subtraction (see Theory). Choice of equal-area (under difference decay function) windows simply saves time. For example, a pair of time windows was chosen to contain equal amounts of HLADH complex contribution. The earlier difference TRES of this pair naturally contains more β-cyclodextrin contributions. When the later difference TRES is subtracted, one obtains a spectrum characteristic of TNS/cyclodextrin *alone*. This is evinced by the fast-rotor ADAS in Figure 3, clearly superposing the pure TNS/cyclodextrin spectrum (taken separately). The correct recovery of spectra for both fast- and slow-rotor populations in this mixture shows two things: first, that time-resolved anisotropy can be used just as well as total decay to "sort out" spectra in a mixture; and second, that coexisting total decay differences can be practically set aside in some systems, since the larger rotational disparity dominates the difference decay function.

Two asides are in order. First, note the presence of a small misfit near 410 nm. This may be attributed to a (Raman) scatter band, seen also in unlabeled samples, whose intensity and polarization are both δ-function images of the excitation pulse. For a discussion of isolating scattered-light terms, see Knutson et al. (1985). The second aside concerns the form of the mixing matrix used:

$$\mathbf{M}_{ij} = \begin{vmatrix} A & A \\ B & 0 \end{vmatrix} \tag{18}$$

A represents the equal areas (under the HLADH complex curve Y_1) in early and late windows, while B is the β-cyclodextrin (Y_2) contribution in the early window. The inverse of $\mathbf{M}_{ij}$, using the convention of products over first (row) index used under Theory, is

$$\begin{vmatrix} 0 & B^{-1} \\ A^{-1} & -B^{-1} \end{vmatrix} \tag{19}$$

Thus, as explained previously, the slow-rotor spectrum is

$$\alpha_1(\lambda) = (0)(\text{early } \Delta\text{TRES}) + (1/A)(\text{late } \Delta\text{TRES}) \tag{20}$$

and the fast-rotor ADAS is

$$\alpha_2(\lambda) = (1/B)(\text{early } \Delta\text{TRES}) - (1/B)(\text{late } \Delta\text{TRES}) \tag{21}$$

Since $1/A$ and $1/B$ are constants, they can be divided out for peak-normalized comparisons like Figure 3.

The point of this aside is to phrase the matrix operations in terms of more familiar spectral subtractions. The advantages of matrix methods become more apparent, however, when three or more components are unmixed. In any case, the matrices are made up of wavelength-invariant elements, so only the last (remixing) step is applied to whole spectra. ADAS may also be obtained from emission anisotropy decay curves at discrete wavelength intervals. These decays can be processed as indicated above or by global methods (Beechem et al., 1984a).

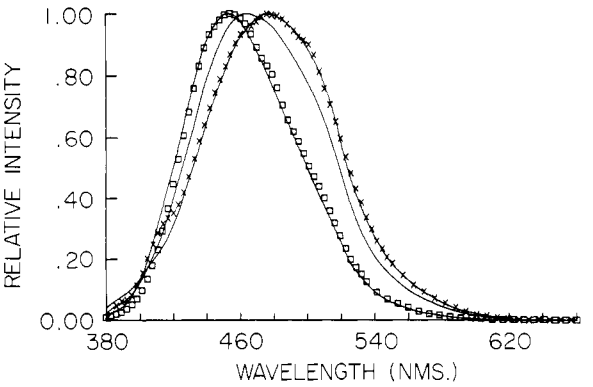

FIGURE 3: Anisotropy decay associated spectra for the TNS/LADH and TNS/cyclodextrin mixtures at 10 °C. The left-most solid line is the steady-state emission spectrum for TNS bound to protein. The longest wavelength curve is the emission spectrum for TNS absorbed to cyclodextrin. The central solid line is the spectrum obtained by mixing the TNS-labeled protein and carbohydrate to give equal emission intensities at the respective emission wavelengths. The late difference spectrum (□) superimposes with the spectrum of the more slowly rotating protein-bound TNS molecules. The ADAS for the more mobile fraction of the mixture (×) also correctly identifies its origins. It was obtained by subtraction of a "late" difference spectrum from an "early" difference spectrum. The mixing coefficients for the "immobile" fraction of fluorophores were equal (for this example) in both time-gated windows. Excitation was 357 nm with excitation and emission bandwidths of 14 and 16 nm, respectively.

Discussion

Biological systems are often made up of subunits of varied size and shape. If one wishes to study either the extrinsic or the intrinsic fluorescence of complex systems, it will be useful to identify any spectral heterogeneity in the system. This is especially applicable when one can assign spectra to components of different size (or shape, or residing in a different viscous environment). Unlike other (more invasive) methods, it is possible to apply fluorescence spectroscopy to intact macromolecular assemblies. The only bar to its use is the complexity of signals obtained along any axis (polarization vs. time vs. wavelength etc.). The complexity becomes manageable when one spreads the information across a surface by exploiting *associations* between parameters. Multidimensional analyses of fluorescence data are becoming more widespread; this will facilitate the study of biochemical heterogeneity. The technique described above should also apply to fluorescence *images* of large assemblies or whole tissues.

Acknowledgments

We thank R. E. Dale, I. Z. Steinberg, and J. M. Beechem for helpful discussion. D. G. Walbridge provided expert technical assistance, and Julie Kang typed the manuscript.

References

Ainsworth, S. (1961) *J. Phys. Chem. 65*, 1968–1972.

Badea, M. G., & Brand, L. (1979) *Methods Enzymol. 61H*, 378–394.

Beechem, J. M., Knutson, J. R., & Brand, L. (1983a) *Photochem. Photobiol. 37*, S20.

Beechem, J. M., Knutson, J. R., Ross, J. B. A., Turner, B. W.,

& Brand, L. (1983b) *Biochemistry 22*, 6054–6058.
Beechem, J. M., Knutson, J. R., & Brand, L. (1984a) *Biophys. J. 45*, 127a.
Beechem, J. M., Ameloot, M., DeToma, R. P., & Brand, L. (1984b) *Biophys. J. 47*, 318a.
Beechem, J. M., Knutson, J. R., & Brand, L. (1985a) *Biophys. J. 47*, 411a.
Beechem, J. M., Ameloot, M., & Brand, L. (1985b) *Chem. Phys. Lett. 120*, 466–472.
Brand, L., Knutson, J. R., Davenport, L., Beechem, J. M., Dale, R. E., Walbridge, D. G., & Kowalczyk, A. A. (1985) in *Spectroscopy and Dynamics of Molecular Biological Systems: Some Applications of Associative Behavior to Studies of Proteins and Membranes* (Bayley, P., & Dale, R. E., Eds.) Academic Press, New York.
Chen, L., Dale, R. E., Roth, S., & Brand, L. (1977) *J. Biol. Chem. 252*, 2163–2166.
Chen, R. F., & Bowman, R. L. (1965) *Science (Washington, D.C.) 147*, 729–731.
Chuang, T. J., & Eisenthal, K. B. (1972) *J. Chem. Phys. 57*, 5094.
Cross, A. J., Waldeck, D. H., & Fleming, G. R. (1983) *J. Chem. Phys. 78 (11)*, 6455–6467.
Davenport, L., & Brand, L. (1985) *Biophys. J. 47*, 367a.
Davenport, L., Knutson, J. R., & Brand, L. (1982) *Am. Soc. Photobiol. 10*, 59A.
Davenport, L., Knutson, J. R., & Brand, L. (1983) *Biophys. J. 41*, 373a.
Davenport, L., Knutson, J. R., & Brand, L. (1986) *Biochemistry 25*, 1186–1195.
Donzel, B., Gauduchon, P., & Wahl, Ph. (1974) *J. Am. Chem. Soc. 96*, 801.
Ermolaev, V. L., Kotlyar, I. P., Lyubimtsev, V. A., & Maslov, V. G. (1982) *Opt. Spectrosc. (Engl. Transl.) 52*, 1.
Gratton, E., Jameson, D. M., & Hall, R. D. (1984a) *Annu. Rev. Biophys. Bioeng. 13*, 105–125.
Gratton, E., Limkeman, M., Lakowicz, J. R., Maliwal, B. P., Cherek, H., & Laczko, G. (1984b) *Biophys. J. 46*, 479–486.
Halvorson, H. R. (1981) *Biophys. Chem. 14*, 177–184.
Jablonski, A. (1960) *Bull. Acad. Pol. Sci., Ser. Sci., Math., Astron. Phys. 8*, 259–264.
Kinosita, K., Kawato, S., & Ikegami, A. (1977) *Biophys. J. 20*, 289.
Knutson, J. R., & Lakowicz, J. R., (1980) *Biophys. J. 29*, 102a.
Knutson, J. R., Walbridge, D. G., & Brand, L. (1982a) *Biochemistry 21*, 4671–4679.
Knutson, J. R., Davenport, L., & Brand, L. (1982b) *Biophys. J. 37*, 203a.
Knutson, J. R., Beechem, J. M., & Brand, L. (1983) *Chem. Phys. Lett. 102*, 501–504.
Knutson, J. R., Davenport, L., Beechem, J., Walbridge, D., Ameloot, M., & Brand, L. (1986) in *Excited-State Probes in Biochemistry and Biology* (Szabo, A., & Masotti, L., Eds.) Plenum Press, New York.
Lakowicz, J. R. (1984) *Biophys. Chem. 19*, 13–23.
Lakowicz, J. R., & Cherek, H. (1981) *J. Biochem. Biophys. Methods 5*, 19–35.
Lakowicz, J. R., Laczko, G., Cherek, H., Gratton, E., & Limkeman, M. (1984) *Biophys. J. 46*, 463–477.
Lipari, G., & Szabo, A. (1980) *Biophys. J. 30*, 489.
Matayoshi, E. D., Kleinfeld, A. M., & Solomon, A. K. (1979) *Biophys. J. 25*, 168a.
Munro, I., Pecht, I., & Stryer, L. (1979) *Proc. Natl. Acad. Sci. U.S.A. 76*, 55.
Perrin, F. (1934) *J. Phys. Radium 5*, 497.
Perrin, F. (1936) *J. Phys. Radium 7*, 1.
Ross, J. B. A., Schmidt, C. J., & Brand, L. (1981) *Biochemistry 20*, 4369–4377.
Schrager, R. I., & Hendler, R. W. (1982) *Anal. Chem. 54*, 1147–1152.
Wahl, Ph. (1969) *Biochim. Biophys. Acta 175*, 55–58.
Weber, G. (1952) *Biochem. J. 51*, 145.
Weber, G. (1953a) *Adv. Protein Chem. 8*, 415–459.
Weber, G. (1953b) *Discuss. Faraday Soc. 13*, 33–39.
Weber, G. (1961) *Nature (London) 190*, 27–29.
Weber, G. (1973) in *Fluorescence Technique in Cell Biology* (Thaer, A. A., & Sernetz, M., Eds.) pp 415–459, Springer Verlag, New York.
Zannoni, C. (1981) *Mol. Phys. 42*, 1303.